Metabolic Changes in an Animal Model of Amyotrophic Lateral Sclerosis Evaluated by [18F]-FDG Positron Emission Tomography

Bruno Lima Giacobbo
Umea Universitet
Tomás Mediavilla
Umea Universitet
Daniel J. Marcellino
Umea Universitet
Fahad Sultan (fahad.sultan@umu.se)
Umeå University https://orcid.org/0000-0001-9194-9905

Research Article

Keywords: [18F]-FDG, Amyotrophic Lateral Sclerosis, neurodegeneration, metabolism, Positron Emission Tomography

Posted Date: March 22nd, 2021

DOI: https://doi.org/10.21203/rs.3.rs-323644/v1

Metabolic changes in an animal model of Amyotrophic Lateral Sclerosis evaluated by [^{18}F]-FDG positron emission tomography

Bruno Lima Giacobbo[1], Tomás Mediavilla[1], Daniel J. Marcellino[1], Fahad Sultan[1]*

Affiliations:

[1] Department of Integrative Medical Biology, Umeå University, Umeå, Sweden

Corresponding author:

* Fahad Sultan

Department of Integrative Medical Biology

Umeå University, Johan Bures väg 12, 901 87 Umeå, Sweden

E-mail: fahad.sultan@umu.se

Keywords:

[^{18}F]-FDG; Amyotrophic Lateral Sclerosis; neurodegeneration; metabolism; Positron Emission Tomography.

Amyotrophic Lateral Sclerosis (ALS) is a fatal neurodegenerative disorder that mainly affects upper and lower motor neurons that progressively leads to loss of motor function and, eventually, death by respiratory failure. Over 10% of all ALS cases are associated with mitochondrial dysfunction, as observed in humans carrying mutations in the gene encoding for superoxide dismutase-1 (SOD1) that lead to dysfunction in SOD1 and increased oxidative stress and loss of neuronal function (1). Observations in humans with mutations in SOD1 led to the development of transgenic mice that express a mutated human SOD1 variant ($hSOD1^{G93A}$) with high face-validity to motor symptoms related to ALS in humans (2). However, although such mice allowed for greater understanding of disease, many of the molecular mechanisms involved in disease onset and progression remain largely unknown, making mouse-to-human translation of ALS symptoms a constant challenge.

Due to its relationship with $SOD1^{G93A}$-dependent mitochondrial loss of function, it has been proposed that ALS affects the metabolism of the organism as well. Some studies report a higher metabolic rate and energy expenditure in ALS patients (3). Thus, it is not surprising that attempts have been made to understand how the metabolic state of ALS patients is affected by the disease, or whether it is possible to mitigate disease progression by modifying the metabolic pattern of patients. On the other hand, studies have tried to use metabolic dysfunction, such as dyslipidaemia and glucose uptake, as a way of identifying disease patterns to improve diagnosis of ALS in humans (4). In that regard, Positron Emission Tomography (PET) has provided a key role in understanding molecular mechanisms of disease *in vivo* since it is relatively non-invasive. Studies using [^{18}F]-fluorodeoxyglucose ([^{18}F]-FDG) has become increasingly important to investigate ALS-dependent metabolic dysfunction due to its non-invasiveness and its ability to target tissues with high glucose uptake, such as the brain (5).

However, even though several studies using PET in ALS patients were performed to assess the regional distribution of glucose hypometabolism as an early diagnostic criterion (5), research using [^{18}F]-FDG in animal models of ALS is lacking. Due to the high face-validity of transgenic animal models of ALS to human ALS symptoms and the fact that animal models are an extremely important tool to understand

the basic mechanisms of disease, the use of preclinical PET to study the pathophysiology of ALS using highly validated transgenic mice is surprisingly low. Hence, the goal of this study was to evaluate CNS [^{18}F]-FDG uptake as a surrogate of glucose metabolism in mice that express a mutated human SOD1 variant (hSOD1^{G93A}). We imaged glucose metabolism using [^{18}F]-FDG in both male and female mice expressing the SOD1^{G93A} mutation with ALS-like symptoms and compared these animals to age- and gender-matched littermate controls (SOD1^{WT}).

The analysis of the animal weight and injected dose at time of [^{18}F]-FDG PET was performed using GLM (for further details see Supplement Methods). Highly significant between-group differences ($F=28.81$; $p<0.0001$) were found, with post-hoc comparisons indicating that male WT mice weighing significantly more than all other groups, while female ALS mice weighing significantly less when compared with all other groups (Supplementary Table 1). There were no significant differences between the groups regarding age at time of scan or the injected dose administered at the time of scan (all $p>0.05$).

[^{18}F]-FDG uptake showed a marked difference between WT and ALS mice (Figure 1). There was lower uptake of [^{18}F]-FDG in the brain of ALS mice compared to WT littermates. A detailed statistical analysis of SUV-normalized [^{18}F]-FDG uptake using a GEE approach revealed a significant effect of gender for almost all the regions evaluated (Supplementary Table 2), with female mice showing a higher SUV for all significant regions assessed (Main effect of gender: Wald-χ^2 <0.0001). However, the cerebellum, basal forebrain and amygdala showed no significant differences between genders. We observed a significant effect of genotype in the [^{18}F]-FDG SUV uptake (Main effect of genotype: Wald-χ^2 <0.0001) with significant differences found in hippocampus, thalamus, midbrain, and right inferior colliculus, with a lower SUV uptake in SOD1^{G93A} when compared with WT animals for all the aforementioned regions. When analyzing the interaction between gender and genotype, there was also a significant effect of both factors in general (Gender x genotype interaction: Wald-χ^2 <0.0001). Pairwise comparisons revealed significant differences between WT females and SOD1^{G93A} males in left hippocampus ($p<0.0001$) and left midbrain ($p=0.049$).

Due to a possible influence of weight between ALS and WT mice, [^{18}F]-FDG uptake from each VOI was normalized to the average uptake of the whole brain for each individual. By normalizing the uptake from each VOI to the whole brain, any possible effect of the weight difference between groups is eliminated. Thus, we compared the tissue-to-reference ratio (TRR) from all regions assessed. TRR analysis showed that the gender differences found in SUV for all regions evaluated disappeared except for right striatum. When the main effect of genotype was analyzed, there were significant differences between WT and SOD1^{G93A} animals in hippocampus, thalamus, olfactory bulb, midbrain, and right inferior colliculus (Supplementary Table 3).

The goal of this study was to evaluate the effects of hSOD1^{G93A} mutation on glucose metabolism in the brain using 10-minute [^{18}F]-FDG PET. The hSOD1^{G93A} animal model of ALS shows a reliable face validity to many human ALS forms with regard to symptom onset and progression, thereby providing a valuable animal model to further understand the pathophysiology of disease and its progression, as well as helping to find promising biomarkers and therapeutic targets that can be used in ALS. In that regard, we found significant changes in glucose metabolism in the brain of SOD1^{G93A} animals when compared with WT control littermates, indicating a change in metabolic pattern in these animals. To the best of our knowledge, this is the first study to detect and quantify the effects of ALS phenotype on brain glucose uptake in mice using non-invasive PET. To specifically investigate early changes in CNS, we scanned animals that were at an initial stage of disease, stage 1 (6), see also Supplement Methods.

The effects of ALS on metabolic function in humans and in animal models of ALS are yet to be fully understood. In animals, only one study has measured the impact of SOD1^{G93A} genotype on glucose uptake using [^{18}F]-FDG, however focus was specifically placed onto metabolic changes in skeletal muscles (7). Marini *et al*. found that mice expressing mutant SOD1^{G93A} had a higher [^{18}F]-FDG uptake in quadriceps when compared with WT animals, indicative of a higher metabolic rate. These changes were accompanied by increased inflammatory profiles and mitochondrial dysfunction in muscle (7). In

humans, however, the assessment of brain metabolism in ALS patients with [^{18}F]-FDG PET has been studied with a focus on prediction of ALS onset and characterization of disease progression, both with mixed results (5). In humans, PET [^{18}F]-FDG studies report a widespread change in brain glucose uptake. Several of these studies point towards a decrease in [^{18}F] FDG PET uptake in primary motor and other premotor regions , while also showing hypermetabolic regions, such as in the limbic system, brainstem, and cerebellum, irrespective of ALS onset type (*i.e.*: bulbar- or spinal-onset ALS) (4). The hypometabolism in frontal regions was explained with the "dying forward" hypothesis of ALS (8) leading to a reduction in glutamatergic cortico-cortical neurotransmission which has a major effect on glucose consumption. Our observation of early reductions in glucose uptake suggests that hypometabolism can also occur prior to such changes in neurotransmission and can be due to an overall hypometabolic state in ALS.

Hypometabolism was also described in other brain regions in humans. van Laere and colleagues observed a significant thalamic hypometabolism (5). In our study, we found a 12% decrease in thalamic [^{18}F]-FDG PET uptake – normalized to the whole brain – supporting the findings of van Laere and colleagues. Interestingly, these changes in thalamic uptake appear to be specific for fALS as recently proposed from observations in a study of carriers of C9orf72 gene (9). However, it is not entirely clear whether specific thalamic nuclei play a key role in onset of ALS, or whether hypometabolism of thalamus is associated to overall reductions in the relay of motor and sensory information throughout the brain.

Two additional regions with significant changes in uptake of [^{18}F]-FDG in WT and SOD1^{G93A} were hippocampus and midbrain. We observed a bilateral decrease in metabolic activity for both regions, in SUV and TRR (Supplementary Table 1 and 2, respectively). Interestingly, human data predominantly report a hypermetabolic state in hippocampus and midbrain, whether by PET or through the use of additional *in vivo* techniques (9). Structural MRI data, on the other hand, suggest a relative decrease in hippocampal volume in ALS patients and loss of hippocampus-dependent cognitive functions (3),

with similar atrophy observed in midbrain. One of the hypothesized origins for such increased metabolism in these areas is an increase in reactive gliosis from oxidative stress and neurotoxicity. In fact, one study performed in SOD1^{G93A} rats report increased gliosis in hippocampus and in brainstem prior to the development of ALS-like symptomatology (10), suggesting that a hypermetabolic state of hippocampus might occur at earlier stages of disease that later decline over time to a hypometabolic state as disease progresses. In order to confirm such hypothesis, future imaging studies in animal models of ALS would require longitudinal scans at a prodromal stage and at several later time points.

Abbreviations

ALS: Amyotrophic Lateral Sclerosis

[^{18}F]-FDG: [^{18}F]-fluorodeoxyglucose

GEE: Generalized Estimating Equations

GLM: Generalized Linear Models

PET: Positron Emission Tomography

PVC: partial volume effects

SOD1: superoxide dismutase-1

SUV: standardized uptake values

TRR: Tissue to reference ratio

VOI: volume of influence

WT: wild-type

Declarations

Ethics approval and consent to participate

All experimental procedures were conducted in accordance with the Umeå University's animal ethical committee (Ethical permit number: 5.2.18-19236/17).

Consent for publication

Not applicable.

Availability of data and materials

The datasets used during the current study are available from the corresponding author on reasonable request.

Competing interests

The authors declare that they have no competing interests.

Funding

BG was funded by a Kempestiftelserna grant to DM and FS. This study was also supported by the Department of Integrative Medical Biology, Umeå University (DM and FS) and from Umeå University Medical Faculty (DM).

Authors' contributions

BG designed the study, collected, and analyzed the data, and prepared the manuscript. TM participated in the data collection and preparation of the manuscript. DM participated in study design and preparation of the manuscript. FS participated in the study design, and preparation of the manuscript.

Acknowledgements

The authors would like to acknowledge Thomas Brännström for providing the initial ALS SOD1^{G93A} breeding pairs to establish a cohort for the performing of this study. The authors would also like to acknowledge the support from Madelene Ericsson and Jan Axelsson on the development of the PET protocol, as well as the support in data analysis. Lastly, the authors would like to acknowledge the Small Animal Research and Imaging Facility (SARIF) at Umeå University for providing the equipment and technical support for performing the study.

Reference list

1. Hardiman O, Al-Chalabi A, Chio A, Corr EM, Logroscino G, Robberecht W, et al. Amyotrophic lateral sclerosis. Nat Rev Dis Primers. 2017;3:17071.
2. Gurney ME, Pu H, Chiu AY, Dal Canto MC, Polchow CY, Alexander DD, et al. Motor neuron degeneration in mice that express a human Cu,Zn superoxide dismutase mutation. Science. 1994;264(5166):1772-5.
3. Vandoorne T, De Bock K, Van Den Bosch L. Energy metabolism in ALS: an underappreciated opportunity? Acta Neuropathol. 2018;135(4):489-509.
4. Dodge JC, Treleaven CM, Fidler JA, Tamsett TJ, Bao C, Searles M, et al. Metabolic signatures of amyotrophic lateral sclerosis reveal insights into disease pathogenesis. Proceedings of the National Academy of Sciences. 2013;110(26):10812-7.
5. Van Laere K, Vanhee A, Verschueren J, De Coster L, Driesen A, Dupont P, et al. Value of 18fluorodeoxyglucose-positron-emission tomography in amyotrophic lateral sclerosis: a prospective study. JAMA Neurol. 2014;71(5):553-61.
6. Hatzipetros T, Kidd JD, Moreno AJ, Thompson K, Gill A, Vieira FG. A Quick Phenotypic Neurological Scoring System for Evaluating Disease Progression in the SOD1-G93A Mouse Model of ALS. J Vis Exp. 2015(104).
7. Marini C, Cossu V, Bonifacino T, Bauckneht M, Torazza C, Bruno S, et al. Mechanisms underlying the predictive power of high skeletal muscle uptake of FDG in amyotrophic lateral sclerosis. EJNMMI Res. 2020;10(1):76.
8. Baker MR. ALS—dying forward, backward or outward? Nature Reviews Neurology. 2014;10(11):660-.
9. Cistaro A, Pagani M, Montuschi A, Calvo A, Moglia C, Canosa A, et al. The metabolic signature of C9ORF72-related ALS: FDG PET comparison with nonmutated patients. Eur J Nucl Med Mol Imaging. 2014;41(5):844-52.
10. Stamenkovic S, Ducic T, Stamenkovic V, Kranz A, Andjus PR. Imaging of glial cell morphology, SOD1 distribution and elemental composition in the brainstem and hippocampus of the ALS hSOD1(G93A) rat. Neuroscience. 2017;357:37-55.

Figure legend

Figure 1: A, B: Sagittal plane of whole body [^{18}F]-FDG representative image of a WT and ALS animal, respectively. Color scale bar indicate radiotracer uptake normalized for injected dose and weight (SUV). **C-D**: Horizontal plane of the head in cropped SUV images. From left to right: an individual head cropped image; an individual brain-masked image; group-based average image; and VOI placement for data analysis. Color scale bar indicate radiotracer uptake normalized for injected dose and weight (SUV). **E-F**: Horizontal plane of the head with radioactivity normalized to the average radioactivity in the whole brain (TRR). From left to right: an individual head cropped image; an individual brain-masked image; group-based average image; and VOI placement for data analysis. Color scale bar indicate radiotracer uptake normalized for averaged radioactivity in whole brain.

Figures

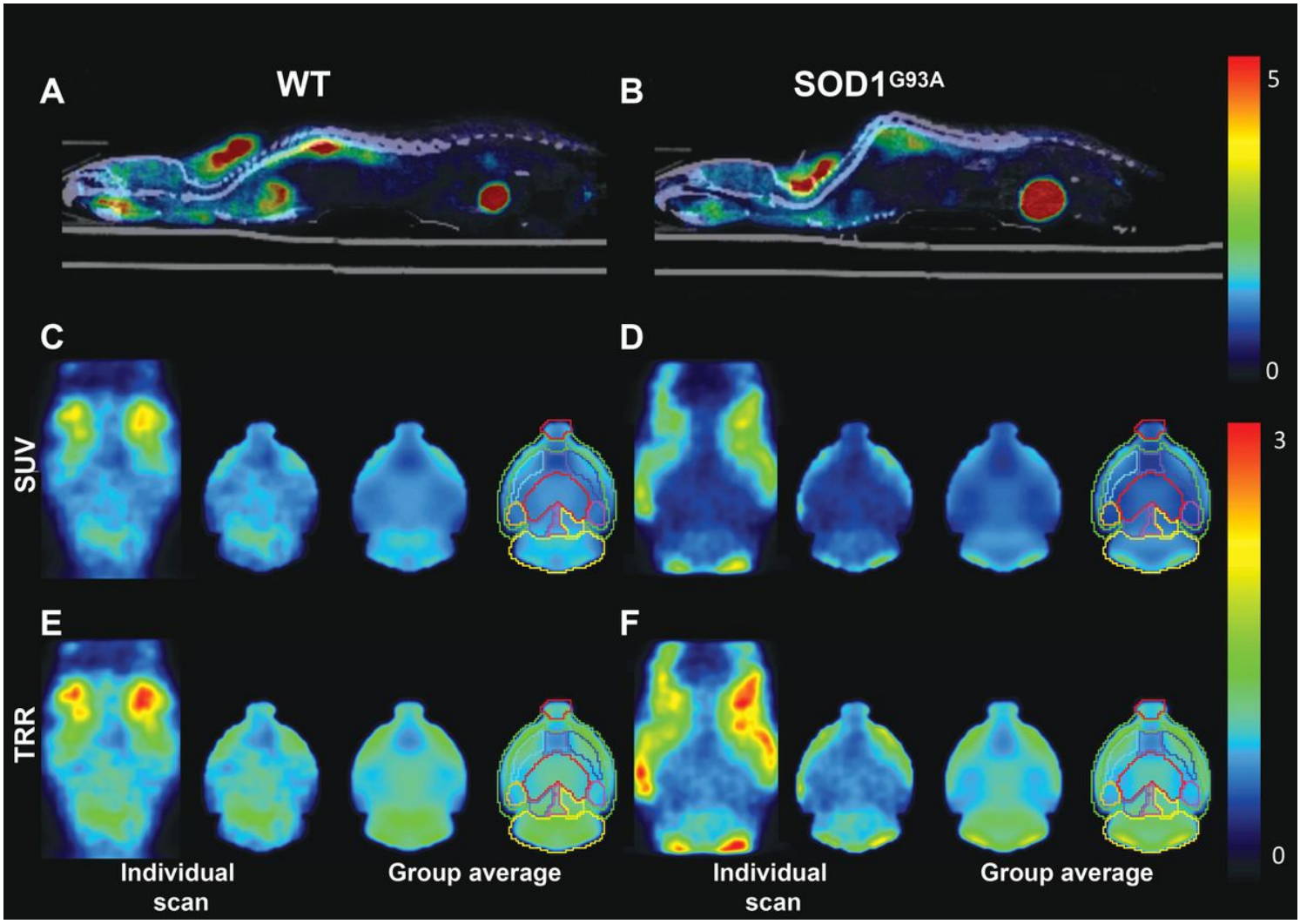

Figure 1

A, B: Sagittal plane of whole body [18F]-FDG representative image of a WT and ALS animal, respectively. Color scale bar indicate radiotracer uptake normalized for injected dose and weight (SUV). C-D: Horizontal plane of the head in cropped SUV images. From left to right: an individual head cropped image; an individual brain-masked image; group-based average image; and VOI placement for data analysis. Color scale bar indicate radiotracer uptake normalized for injected dose and weight (SUV). E-F: Horizontal plane of the head with radioactivity normalized to the average radioactivity in the whole brain (TRR). From left to right: an individual head cropped image; an individual brain-masked image; group-based average image; and VOI placement for data analysis. Color scale bar indicate radiotracer uptake normalized for averaged radioactivity in whole brain.

Supplementary Files

This is a list of supplementary files associated with this preprint. Click to download.

- BGLSOD1ALSFDGSupplementarymaterial.docx